International Journal of Information, Control and Computer Sciences
ISSN: 2517-9942
Vol:9, No:12, 2015

3D Liver Segmentation from CT Images Using a Level Set Method Based on a Shape and Intensity Distribution Prior

Nuseiba M. Altarawneh, Suhuai Luo, Brian Regan, Guijin Tang

***Abstract*—**Liver segmentation from medical images poses more challenges than analogous segmentations of other organs. This contribution introduces a liver segmentation method from a series of computer tomography images. Overall, we present a novel method for segmenting liver by coupling density matching with shape priors. Density matching signifies a tracking method which operates via maximizing the Bhattacharyya similarity measure between the photometric distribution from an estimated image region and a model photometric distribution. Density matching controls the direction of the evolution process and slows down the evolving contour in regions with weak edges. The shape prior improves the robustness of density matching and discourages the evolving contour from exceeding liver's boundaries at regions with weak boundaries. The model is implemented using a modified distance regularized level set (DRLS) model. The experimental results show that the method achieves a satisfactory result. By comparing with the original DRLS model, it is evident that the proposed model herein is more effective in addressing the over segmentation problem. Finally, we gauge our performance of our model against matrices comprising of accuracy, sensitivity, and specificity.

***Keywords*—**Bhattacharyya distance, distance regularized level set (DRLS) model, liver segmentation, level set method.

I. Introduction

LIVERS constitute one of the most prominent organs in our bodies. It performs key functions including cleaning blood from impurities, producing bile and proteins, treating sugar, decomposition of medications, and storing valuable nutrients such as iron, minerals and vitamins. As a result of high functionality, the liver is prone to many notorious diseases such as hepatitis C, cirrhosis, and cancer. With the very rapid advancement in computer science and its associated technology, computer-aided surgical planning systems (CAD) continue to play an important role in diagnosis and treatment of the aforementioned liver diseases. These promising approaches can map out the structures of various liver vessels, afford accurate 3D visualizations, and provide surgical insights of simulations with cutting. All these applications have the potential to lead to shorter planning times. One of the most daunting tasks in the context of computer tomography (CT) images is to carry out an automatic and accurate segmentation of a liver from its surrounding organs. Establishing an effective methodology for liver segmentation from CT images proves to be a challenging mission. This is mainly due to the profoundly similar intensity values between liver and its adjacent organs. Other contributing factors include artifacts of pulsation and motion and partial volume effects. The substantial variations in shape and volume of liver among people even add more hurdles toward accurate segmentation of the liver. It follows that liver segmentation from medical images still pose an interesting theme of research.

Methods and approaches currently implemented in liver segmentation in the CT images are grouped into two main families: semiautomatic and fully automatic liver segmentation methods. Semi-automatic liver segmentation methods necessitate a limited user intervention. This intervention could be a manual selection of seed points or a manual refinement of a binary mask for the liver. The term fully automated refers to a liver segmentation process that is implemented without any sort of operator intervention. As a consequence, this method is highly regarded by radiologists as it is free from user errors and biases. The advantage herein is that this method requires less operational work and saves time. Subsequent discussion is based into categorizing liver segmentation methods into gray level based methods, model based methods, and texture based methods [1]. It is obvious that each category will incur its own advantages and drawbacks.

The gray level based methods [2]-[13] abstracts image features directly. This important property makes gray level based methods to be the most commonly deployed methods in liver segmentation. These methods are mainly based on the evolution of the gray level toward targets. Whilst gray level methods are normally fast, their effectiveness may be limited, most notably when gray level intensity of targets display changes. Despite of the deployment of prior knowledge, gray level methods may not succeed when the liver is represented as a small fraction of the entire image. Gray level methods can either be applied manually or through automatic rough segmentation. The goal of these two procedures is to gather data pertinent to the gray level. In spite of their reliability, gray level methods often need excessive computational time. Numerous gray level based methods rely on gradient information as an accurate approach to deal with image boundaries. However, this approach becomes impractical in the presence of complexity and several boundaries in which only some of them are the real boundaries of the desired object.

Nuseiba M. Altarawneh, Suhuai Luo, Brian Regan is with School of Des, Australia (e-mail: nuseiba.altarawnh@uon.edu.au, suhuai.luo@newcastle.edu.au, brian.regan@newcastle.edu.au)
Guijin Tang is with College of Telecommunication & Information Engineering, Nanjing University of Posts and Telecommunications, Nanjing 210003, China (e-mail: tanggj@njupt.edu.cn).ign, Communication and IT, the University of Newcastle, Callaghan NSW 2308

Under these circumstances, gray level based methods may potentially converge into incorrect boundaries, i.e. producing over or under segmentation. However, this could be readily corrected by refining the results through manual operations or via implementing other methods. On the contrary, structure based methods [14]-[17] can effectively deal with unclear liver boundaries through utilizing prior knowledge. However, these methods often demand substantial training data to account for all probable conditions of the liver. Implementing these methods is associated with significant difficulty, especially when handling nonstandard liver shapes. It is very difficult to develop a unified segmentation model for the liver based merely on structure methods. Texture based methods [18], [19] deploys pattern recognition and machine learning principles to locate boundaries of a liver. As a result, these methods enable one to collectively consider more features. Texture based methods can yield satisfactory results when the boundaries are not very clear. In addition to its dependency on training data, an accurate account of texture feature remains the main challenges in these methods. While many descriptors do exist, they could not accurately resemble corresponding descriptors in humans. It is worthwhile mentioning that both machine learning and pattern recognitions are still immature technologies with lesser ability to process information when compared with the human brain. They are not able to produce satisfactory segmentation results without the aid of other refined methods. In contrast, gray level based methods are more highly advanced as they can effectively deal with complex segmentation tasks.

In most practical cases, gray level based methods can yield satisfactory performance in liver segmentation. Structure based methods rely principally on the shape of the object. This characteristic enables them to be a significantly more robust technique. Lastly, texture based methods attempt to follow the procedure that a human's brain implements. Level set methods have been thoroughly deployed in medical images segmentation [20]-[22] However, these methods attain good results only when the initial contour is positioned near the target. In dealing with volumetric liver segmentation, methods can be classified into two groups, i.e., direct 3D segmentation and propagation of the 2D slice-based segmentation. In the first class, the user initializes a 3D deformable surface in terms of multiple 2D slices of the liver. In the approach, the initial 3D mesh is automatically refined by forces imposed by the image gradient and smoothness of the contour. As a result, these methods are timely consuming and require many user interventions, i.e., they are prone to observer variability. The second class of methods takes advantage of the slice-based propagation approach. In this methodology, the 3D CT images are further re-sliced into a number of 2D slices. A 2D segmentation is deployed in each slice. The latter is initialized by a propagated boundary from the previous 2D slice, and hence the process repeats itself. In other words, this approach reduces a 3D segmentation problem to a sequence of 2D segmentation problems. Each of the reduced 2D segmentation sub-problems is significantly simpler than the original 3D segmentation problem. Furthermore, it is significantly computationally cheaper to incorporate 2D shape data as a shape constraint into the 3D segmentation process. Since the change between adjacent slices is rather small, the final contour of a slice affords useful information with regard to the initial contour position and prior intensity and shape information. This in turn improves the segmentation performance of the level set method for the following slices.

In our underlying goal is to segment the liver contour in each 2D slice by utilizing a new force that guides the direction of the evolution and slows down the evolution process in the region with weak edges or without edges. This paper is organized as follows. In Section II, we survey literature pertinent to the methodology of the DRLS model. Section III illustrates our methodology. Section V presents experimental results. Finally, Section V conveys concluding remarks.

II. Distance Regularized Level Set Method

Li et al. [23] introduced the level set method of distance regularized level set (DRLS) model. The DRLS model utilizes an edge-based active contour method in order to direct the level set function (LSF) to the desired boundary. This method is known to provide a simple and effective narrowband implementation without requiring re-initialization.

Let $\phi:\Omega\to\Re$ be a level set function defined over the domain Ω, then the energy function $\varepsilon(\phi)$ can be expressed as:

$$\varepsilon(\phi)=\beta R_p(\phi)+\varepsilon_{ext}(\phi) \tag{1}$$

where $\beta>0$ is a constant and $R_p(\phi)$ denotes the level set regularization term, identified by:

$$R_p(\phi)=\int_\Omega p(|\nabla\phi|)dx \tag{2}$$

where p stands for an energy density function $p:[0,\infty)\to\Re$, defined as

$$p(s)=\begin{cases}\frac{1}{2}(s-1)^2, & \text{if } s>1\\ \frac{1}{(2\pi)^2}(1-\cos(2\pi s)), & \text{otherwise}\end{cases} \tag{3}$$

Minimization of the energy $\varepsilon(\phi)$ can be attained by solving a level set evolution equation. For a LSF, an external energy function can be formulated as:

$$\varepsilon_{ext}(\phi)=\lambda L_g(\phi)+\alpha A_g(\phi) \tag{4}$$

where λ and α are the coefficient of the length term $L_g(\phi)$ and area term $A_g(\phi)$, which is given by

$$L_g(\phi)=\int g\delta_\varepsilon(\phi)|\nabla\phi|\,dx \tag{5}$$

and

$$A_g(\phi)=\int gH_\varepsilon(-\phi)dx \tag{6}$$

where $g \in [0,1)$ is an edge indicator function given by

$$g = \frac{1}{1 + \left|\nabla G_\sigma * I\right|^2} \tag{7}$$

In this equation G_σ is a Gaussian kernel with a standard deviation σ, and I is the input image. In (5) and (6), the Dirac delta function δ_ε and the Heaviside function H_ε are approximated by the following smooth functions δ_ε and H_ε, respectively. This follows the general procedure in several level set methods:

$$\delta_\varepsilon(s) = \begin{cases} \frac{1}{2\varepsilon}[1+\cos(\frac{\pi t}{\varepsilon})], & \text{if } |t| \le \varepsilon \\ 0, & \text{otherwise} \end{cases} \tag{8}$$

and

$$H_\varepsilon(s) = \begin{cases} \frac{1}{2}(1+\frac{t}{\varepsilon}+\frac{1}{\pi}\sin(\frac{\pi t}{\varepsilon})), & \text{if } |t| \le \varepsilon \\ 0, & \text{if } t < -\varepsilon \\ 1, & \text{if } t > \varepsilon \end{cases} \tag{9}$$

In (8) and (9), ε is a constant, typically set to 1.5. The length term $L_g(\phi)$ was initially introduced by Caselles et al. [24] in their developed geodesic active contour (GAC) model. $L_g(\phi)$ estimates the line integral of the function g along the zero level contour of ϕ. $L_g(\phi)$ is minimized upon the existence of the zero level set of ϕ at the object boundaries. As such, it maintains the curve smooth throughout the deformation process. The area term $A_g(\phi)$ computes the weighted area enclosed within the evolving contour. It aims to speed up the motion of the zero level contour when the contour is not close to the desired object boundaries and to slow down the expanding and shrinking of the zero level contour when it approaches the object boundaries. $A_g(\phi)$ introduces a balloon forces whereas the sign of α guides the direction of the level set evolution, either through its shrinking or expanding. Finally, the level set evolution equation in the DRLS model is expressed by:

$$\frac{\partial \phi}{\partial t} = \beta.\mathrm{div}(d_p(|\nabla\phi|)\nabla\phi) + \delta(\phi).\lambda.\mathrm{div}\left(g\frac{\nabla\phi}{|\nabla\phi|}\right) + \delta(\phi).\alpha.g \tag{10}$$

The main drawback with the DRLS model in the case of liver segmentation is that the curve evolves and deviates from the liver boundary at the region with weak edges or without edges. In this work, we will modify the distance regularization level set method [23] (DRLSM). This is achieved by introducing a new force that guides the evolution process and discourages the evolving contour from leaking at a region with weak edges or without edges. This new force also prevents the contour from going far from the liver boundary.

III. The Proposed Method

In this paper, we modify the DRLS model to segment the liver contour in each 2D slice by combining both geometric and photometric information to control the direction of the evolution and slow down the evolution process in the region with weak or edges or without edges, which subsequently discourages the evolving contour from leaking at a region with weak edges or without edges and from deviating from the liver boundary. Our method is based on energy minimization. The energy function consists of two parts, one term is based on image features (E_i) and a second term is based on a shape prior E_s.

$$E = \lambda_3 E_i + (1-\lambda_3)E_s \tag{11}$$

where $\lambda_3 \in [0,1]$ defines the relative weight between E_i and E_s. Smaller E means better matching between the evolving curve and the liver boundary. A curve which minimizes the energy E is taken to be a solution to the problem. The details of the method are described as below.

A. Density Matching

In this paper, we propose to minimize E_i which measures a similarity between the distribution of an image features inside the curve and that of a model distribution learned a priori. We used the Bhattacharyya coefficient [25]-[29] as a similarity measure.

Let $I_X = I(x) : \Omega \subset \mathbb{R}^2 \to Z$ be an image function from the domain Ω to the space Z of a photometric variable with intensity [0-255]. Let $\partial\Gamma/\partial t = \partial E_i/\partial\Gamma$ be a closed planar parametric curve. Our purpose is to evolve Γ in order to divide Ω into two regions: $R_{in} = R_\Gamma$ corresponding to the interior of Γ (foreground), and, $R_{out} = R_{in}^c = R_\Gamma^c$ corresponding to the exterior of Γ (background). The evolution equation of Γ is sought by optimizing a statistical overlap prior. To introduce such prior, we first consider the following definitions:

- P_{in} is the nonparametric (kernel-based) estimate of the distribution of image data inside Γ

$$\forall_z \in Z \quad P_{in(z)} = \frac{\int_{R_{in}} k(z - I_x)dx}{A_{in}} \tag{12}$$

where A_{in} is the area of region R_{in}. Typical choices of K are the Dirac function and the Gaussian kernel [26]

$$\mathrm{K}(y) = \frac{1}{\sqrt{2\pi}h^2}\exp^{\frac{-y^2}{2h^2}} \tag{13}$$

- $\mathrm{B}(f/g)$ is the Bhattacharyya coefficient measuring the similarity between two statistical samples f and g:

$$\mathrm{B}(f/g)=\int_{z\in Z}\sqrt{f(z)g(z)} \tag{14}$$

We assume that the image feature inside the liver is characterized by a model distribution *M*, which can be learned priori. We propose to minimize the following energy functional with respect to L.

$$\mathrm{B}(M/P_{in})=\int_{z\in z}\sqrt{M(z)P_{in}(z)} \tag{15}$$

Note that the values of B are always in [0, 1], measuring the closeness of the distributions; that is, larger values of B correspond to more similar distributions. The goal is therefore to maximize B. In order to convert this to the language of energies, we should set $E_i=-\mathrm{B}(M/P_{in})$. E_i can thus be minimized via gradient descent using the following flow:

$$\frac{\partial E_i}{\partial\Gamma(s,t)}=\frac{1}{2A_{out}}\left(B(M(z)P_{in}(z))-\int_{z\in Z}K(z-I_{\Gamma(s,t)})\sqrt{\frac{P_{in}(z)}{M(z)}}dz\right)\times n(s,t) \tag{16}$$

where t is an artificial time parameterizing the descent direction, and $\partial E_i/\partial\Gamma$ denotes the functional derivative of E_i with respect to Γ. This term has a clear interpretation: when the evolving curve reaches the boundary of liver, the distribution of image feature inside the curve approaches the model M. Therefore, both the global measure $B(M(z),P_{in}(z))$ and the pixel wise measure $\sqrt{P_{in}(z)/M(z)}$ become very close to one. This leads $\partial E_i/\partial\Gamma$ to approximately equal to zero.

$$\frac{\partial\phi}{\partial t}(x,t)=[(\frac{\lambda}{2A_{out}}\left(B(M,\phi)-\int_{z\in Z}K(z-I_x)\sqrt{\frac{P_{in}(z)}{M(z)}}dz\right)]\|\nabla\phi(x,t)\| \tag{17}$$

where ϕ is the level set function corresponding to the evolving curve. Since the liver has a very similar intensity with its adjacent organs, the evolving curve may continue evolving to the adjacent organ producing an over segmentation problem. Consequently, this term will not yield a satisfactory result in the case of liver segmentation. To overcome this obstacle, we add another term to prevent the evolving curve from going far in regions with weak edges or without edges. We refer to this term as the shape prior.

B. Shape Prior

In many applications of image segmentation, some knowledge about the shape of expected objects of interest is available. This prior shape information can be introduced into the level set functional and embedded by the signed distance function. In this contribution, we have used the isotropic Gaussian shape prior [30] to improve the robustness of density matching and to discourage the evolving contour from going far away from the liver boundary or from leaking at a region that does not have an edge.

$$E_s(\phi)=\int_{\Omega}(\phi(x)-\phi_0(x))^2dxdy \tag{18}$$

where ϕ is the current evolving curve and ϕ_0 is the prior shape. In our model the shape term represents the difference between two sign distance function (SDF), whereas its minimum will be attend when the two SDF matches each other.

$$\frac{\partial\phi}{\partial t}(x,t)=-(\phi(x)-\phi_0(x))\|\nabla\phi(x,t)\| \tag{19}$$

IV. The Modified DRLSM

The energy function in (1) can be rewritten as:

$$\varepsilon(\phi)=\lambda_1R_p(\phi)+\lambda_2L_g(\phi)+\lambda_3E(\phi) \tag{20}$$

where $E(\phi)$ is

$$E(\phi)=\lambda_3E_i(\phi)+(1-\lambda_3)E_s(\phi)$$

The level set evolution equation in the modified DRLS model is defined by:

$$\frac{\partial\phi}{\partial t}=\lambda_1.\mathrm{div}(d_p(|\nabla\phi|)\nabla\phi)+\delta(\phi).\lambda_2.\mathrm{div}\left(g\frac{\nabla\phi}{|\nabla\phi|}\right)+[(\frac{\lambda_3}{2A_{out}}\left(B(M,\phi)-\int_{z\in Z}K(z-I_x)\sqrt{\frac{P_{in}(z)}{M(z)}}dz\right)-(1-\lambda_3)(\phi_0(x)-\phi(x,t))]\|\nabla\phi(x,t)\| \tag{21}$$

The first term is penalizing energy and it acts as an internal energy to penalize the deviation from a SDF during its evolution. The second term is the edge term and it keeps the curve smooth during the deformation. The third term is the region energy which controls the direction of evolution. Its minimum will be when the distribution inside the curve matches the model distribution. The fourth term is the shape term to discourage the curve from evolving so far in the region with weak edges or without edges. Its minimum will be on the liver boundary.

A. Pre-Processing

The intensity distribution of the liver is irregular due to noises. As a result, liver segmentation without pre-processing becomes a daunting task. A smoothing step, in theory, would make the intensity distribution less variable. In our work, a Gaussian filter is used as a smoothing step.

B. Segmentation of the Reference Slice

This step is the most important step in our 3D liver segmentation method. The segmented liver contour will be the initial contour for the adjacent slice so the segmentation result should be accurate. The starting slice or the reference slice can be selected as the middle or the largest slice of the liver volume. The model distribution M is a learned priori from a pre-segmented training image. To segment the initial slice we evolve the curve a cording the following energy function:

$$\frac{\partial \phi}{\partial t} = \lambda_1 .\mathrm{div}(d_p(|\nabla \phi|)\nabla \phi) + \delta(\phi).\lambda_2 .\mathrm{div}\left(g\frac{\nabla \phi}{|\nabla \phi|}\right) + [(\frac{\lambda_3}{2A_{out}}(B(M,\phi) - \int_{z\in Z} K(z-I_x)\sqrt{\frac{P_{in}(z)}{M(z)}}dz)]\|\nabla \phi(x,t)\| \quad (22)$$

C. 2D Slice Based Propagation Approach

Since the variation of shape and intensity between the adjacent slices are very minimal, we can use this information from the previous slice to segment the next slice. In our method, we estimate the distribution model M and the prior shape ϕ_0 from the previous segmented slice and deploy it as prior information to segment its adjacent slices in both directions according to (21).

V. Result and Discussion

We tested our model on a liver dataset containing 10 volumes of abdominal CT images. Each volume has 64 slices and the size of each slice is 512 × 512 pixels. Each slice in the dataset is provided with corresponding ground truth segmented manually by a radiologist. The model distribution M is to be learned a priori from a pre-segmented training image for one volume of abdominal CT images. In each experiment, we selected values of λ_1, λ_2 and λ_3 to be 0.02, 5 and 0.5 respectively. The zero level set is initialized as a SDF and evolves according (22) to segment the reference slice and (21) to segment all the remaining slices in the liver volume.

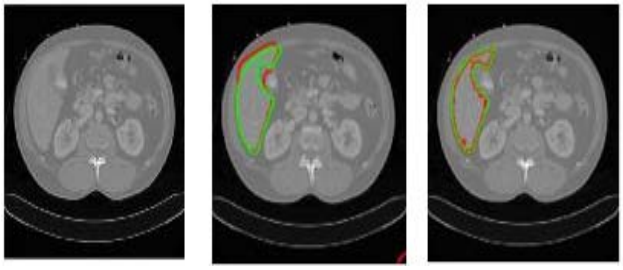

(a) (b) (c)

Fig. 1 Comparisons of liver segmentation results between the DRLS model and the proposed method (a) The liver slice in a CT scan, (b) The final segmentation result of the DRLS model, and (c) The final segmentation result with our proposed method (The final evolving contour in red and ground truth segmented manually by a radiologist is represented in green)

Figs. 1 and 2 present segmentation results of the DRLS model and the proposed model in a liver CT slice. Our model performs well and gives a satisfactory result comparing to the DRLS model. The DRLS model fails to segment the liver boundary and the evolving contour leaks from the region with weak edges. Our method slows down the evolution process close to the liver boundary and prevents the evolving contour from going far in the region with weak edges or without edges. Comparing with the DRLS model, our model is more effective in dealing with over-segmentation problem.

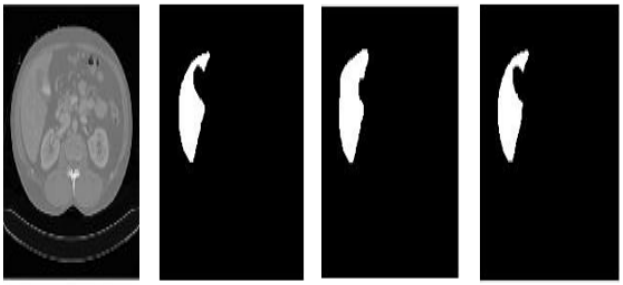

(a) (b) (c) (d)

Fig. 2 Comparisons of liver segmentation result between the DRLS model and the proposed method (a) The liver slice in a CT scan, (b) The ground truth segmented manually by a radiologist, (c) The final segmentation result of the DRLS model and (d) shows the final segmentation result with our proposed method with 99% accuracy

Fig. 3 shows some examples of liver extraction results for one volume of abdominal CT images based on our proposed method. The model deals very well with the over-segmentation problem.

Our model can handle the over-segmentation problems very well in comparison with the DRLS model. We use three metrics to evaluate the segmentation result: accuracy, sensitivity and specificity. The first matrix evaluates the general performance of our method; the second one assesses the acceptance capability of liver tissues and the last one focuses on the rejection capability of non-liver tissues.

Accuracy is defined as:

$$accuracy = \frac{TP + TN}{TP + TN + FP + FN} \quad (23)$$

where *TP* refers to the number of true positive cases; TN is true negative cases; *FP* is false positive cases and FN is false negative cases. Table I defines *TP*, TN, FP and FN.

Sensitivity is defined as:

$$sensitivity = \frac{TP}{TP + FN} \quad (24)$$

Sensitivity term refers to the number of liver tissues that are accepted in the outcome in comparison with ground truth. Lastly, specificity is represented by:

$$specificity = \frac{TN}{TN + FP} \quad (25)$$

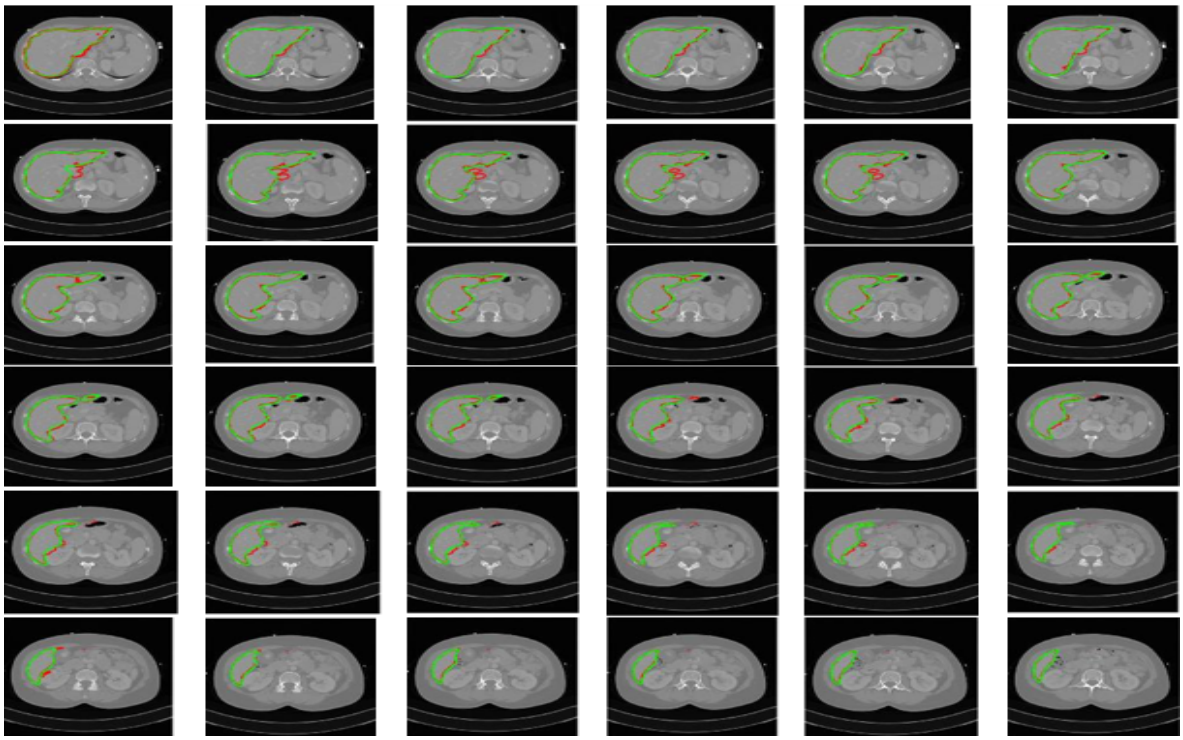

Fig. 3 Experimental results of our proposed method on a sequence of liver slices for one person (The green and red colors refer to the ground truth segmented manually by a radiologist and the final segmentation result of our proposed method, respectively)

TABLE I
THE DEFINITION OF TP, TN, FP AND FN

		Ground truth label	
		Positive	negative
Test outcomes	positive	TP	FP
	negative	FN	TN

TABLE II
PERFORMANCE METRICS OF THE PROPOSED LIVER SEGMENTATION ALGORITHM

accuracy	Average	0.9953
	Standard deviation	0.0030
	Max	0.9995
	Min	0.9888
sensitivity	Average	0.9300
	Standard deviation	0.0455
	Max	0.9959
	Min	0.7988
specificity	Average	0.9980
	Standard deviation	0.0018
	Max	1
	Min	0.9922

Specificity term signifies the number of non-liver tissues that are rejected in the outcome. The result shows that our method achieves high accuracy, specificity, and sensitivity. In reference with regularized level set method, our method shows more effectiveness on the unclear boundary cases. Figs. 1 and 2 reveal that when the boundary between liver and around tissues is not clear, regularized level set leads to over-segmentation whereas our method stops at the boundary. Table II shows the performance metrics of the proposed method.

VI. CONCLUSION

A novel method is presented herein to extract the liver from the CT images using shape and density prior information with a high accuracy. The main merits of this approach are characterized by its profound ability to guide the direction of the evolving contour and to slow down the evolving contour in regions that are associated with weak edges or without edges. Furthermore, in the proposed model the evolving contour is prevented from going far away from the liver boundary or from leaking at regions with weak or no edges. The experimental results illustrate that the method generally attains satisfactory results in reference to the original DRLS model.

ACKNOWLEDGMENTS

The author, Nuseiba M. Altarawneh, thanks the University of Newcastle for the award of a research scholarship.

REFERENCES

[1] S. Luo, X. Li, and J. Li, "Review on the Methods of Automatic Liver Segmentation from Abdominal Images," *Journal of Computer and Communications,* vol. 2, p. 1, 2014.
[2] R. Adams and L. Bischof, "Seeded region growing," *Pattern Analysis and Machine Intelligence, IEEE Transactions on,* vol. 16, pp. 641-647, 1994.
[3] A. Beck and V. Aurich, "Hepatux–a semiautomatic liver segmentation system," *3D Segmentation in The Clinic: A Grand Challenge,* pp. 225-233, 2007.
[4] R. Pohle and K. D. Toennies, "Segmentation of medical images using adaptive region growing," in *Medical Imaging 2001*, 2001, pp. 1337-1346.

[5] K. J. Mortelé, V. Cantisani, R. Troisi, B. de Hemptinne, and S. G. Silverman, "Preoperative liver donor evaluation: imaging and pitfalls," *Liver Transplantation,* vol. 9, pp. S6-S14, 2003.
[6] S. Kumar, R. Moni, and J. Rajeesh, "Automatic liver and lesion segmentation: a primary step in diagnosis of liver diseases," *Signal, Image and Video Processing,* vol. 7, pp. 163-172, 2013.
[7] C. Platero, J. M. Poncela, P. Gonzalez, M. C. Tobar, J. Sanguino, G. Asensio*, et al.*, "Liver segmentation for hepatic lesions detection and characterisation," in *Biomedical Imaging: From Nano to Macro, 2008. ISBI 2008. 5th IEEE International Symposium on*, 2008, pp. 13-16.
[8] D. A. B. Oliveira, R. Q. Feitosa, and M. M. Correia, "Liver Segmentation using Level Sets and Genetic Algorithms," in *VISAPP (2)*, 2009, pp. 154-159.
[9] H. Yang, Y. Wang, J. Yang, and Y. Liu, "A novel graph cuts based liver segmentation method," in *Medical Image Analysis and Clinical Applications (MIACA), 2010 International Conference on*, 2010, pp. 50-53.
[10] Y.-W. Chen, K. Tsubokawa, and A. H. Foruzan, "Liver segmentation from low contrast open MR scans using k-means clustering and graph-cuts," in *Advances in Neural Networks-ISNN 2010*, ed: Springer, 2010, pp. 162-169.
[11] A. H. Foruzan, C. Yen-Wei, R. A. Zoroofi, A. Furukawa, H. Masatoshi, and N. TOMIYAMA, "Segmentation of Liver in Low-Contrast Images Using K-Means Clustering and Geodesic Active Contour Algorithms," *IEICE TRANSACTIONS on Information and Systems,* vol. 96, pp. 798-807, 2013.
[12] J. Liu and J. K. Udupa, "Oriented active shape models," *Medical Imaging, IEEE Transactions on,* vol. 28, pp. 571-584, 2009.
[13] N. M. Altarawneh, S. Luo, B. Regan, and C. Sun, "A modified distance reguularized level set model forl liver segmentation from CT images," *Signal & Image Processing,* vol. 6, p. 1, 2015.
[14] T. Heimann, I. Wolf, and H.-P. Meinzer, "Active shape models for a fully automated 3D segmentation of the liver–an evaluation on clinical data," in *Medical Image Computing and Computer-Assisted Intervention–MICCAI 2006*, ed: Springer, 2006, pp. 41-48.
[15] M. Erdt, S. Steger, M. Kirschner, and S. Wesarg, "Fast automatic liver segmentation combining learned shape priors with observed shape deviation," in *Computer-Based Medical Systems (CBMS), 2010 IEEE 23rd International Symposium on*, 2010, pp. 249-254.
[16] H. Badakhshannoory and P. Saeedi, "A model-based validation scheme for organ segmentation in CT scan volumes," *Biomedical Engineering, IEEE Transactions on,* vol. 58, pp. 2681-2693, 2011.
[17] W. Huang, Z. Tan, Z. Lin, G. Huang, J. Zhou, C. Chui*, et al.*, "A semi-automatic approach to the segmentation of liver parenchyma from 3D CT images with Extreme Learning Machine," in *Engineering in Medicine and Biology Society (EMBC), 2012 Annual International Conference of the IEEE*, 2012, pp. 3752-3755.
[18] S. Luo, Q. Hu, X. He, J. Li, J. S. Jin, and M. Park, "Automatic liver parenchyma segmentation from abdominal CT images using support vector machines," in *Complex Medical Engineering, 2009. CME. ICME International Conference on*, 2009, pp. 1-5.
[19] S. Luo, X. Li, and J. Li, "Improvement of Liver Segmentation by Combining High Order Statistical Texture Features with Anatomical Structural Features," *Engineering,* vol. 5, p. 67, 2013.
[20] N. M. Altarawneh, S. Luo, B. Regan, C. Sun, and F. Jia, "global threshold and region-based active contour model for accurate image segmentation."
[21] N. M. Altarawneh and B. Regan, "A novel global threshold-based active contour model," *Computer Science,* 2014.
[22] C. Xu, d. l.pham, and j. l.prince, "Medical Image Segmentation Using Deformable Models," in *SPIE Handbook on Medical Imaging* vol. 3, J. M. Fitzpatrick and M. Sonka, Eds., ed, 2000, pp. 129-174.
[23] C. Li, C. Xu, C. Gui, and M. D. Fox, "Distance regularized level set evolution and its application to image segmentation," *Image Processing, IEEE Transactions on,* vol. 19, pp. 3243-3254, 2010.
[24] V. Caselles, R. Kimmel, and G. Sapiro, "Geodesic active contours," *International journal of computer vision,* vol. 22, pp. 61-79, 1997.
[25] D. Freedman and T. Zhang, "Active contours for tracking distributions," *Image Processing, IEEE Transactions on,* vol. 13, pp. 518-526, 2004.
[26] T. Georgiou, O. Michailovich, Y. Rathi, J. Malcolm, and A. Tannenbaum, "Distribution metrics and image segmentation," *Linear algebra and its applications,* vol. 425, pp. 663-672, 2007.
[27] Y. Rathi, O. Michailovich, J. Malcolm, and A. Tannenbaum, "Seeing the unseen: Segmenting with distributions," in *International conference on signal and image processing*, 2006.
[28] T. Zhang and D. Freedman, "Tracking objects using density matching and shape priors," in *Computer Vision, 2003. Proceedings. Ninth IEEE International Conference on*, 2003, pp. 1056-1062.
[29] I. B. Ayed, S. Li, and I. Ross, "A statistical overlap prior for variational image segmentation," *International journal of computer vision,* vol. 85, pp. 115-132, 2009.
[30] D. Cremers, N. Sochen, and C. Schnörr, "Towards recognition-based variational segmentation using shape priors and dynamic labeling," in *Scale Space Methods in Computer Vision*, 2003, pp. 388-400.